

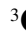



A CASE STUDY ON MODEL PREDICTIVE CONTROL OF THE VLS-1 ATTITUDE AT MAX DYNAMIC PRESSURE

*Antonio Silveira¹, Marco Sagliano², David Seelbinder³, Stephan Theil⁴, João Viana da Fonseca Neto⁵, Rufin Azonsivo⁶, Matheus Moraes da Silva⁶, Marcelo Nunes de Lima⁶, Daniel Abreu Macedo da Silva⁶, Lucas de Carvalho Sodré⁶, and Marco César da Rocha Seruffo⁷

¹  0000-0002-2698-2677, Postgrad. Prog. in Electrical Engineering, Federal University of Pará, Pará, Brazil


²  0000-0003-4579-6121, Department of Navigation and Control, German Aerospace Center, Bremen, Germany

³  0000-0003-4080-3169, Department of Navigation and Control, German Aerospace Center, Bremen, Germany

⁴  0000-0002-5346-8091, Department of Navigation and Control, German Aerospace Center, Bremen, Germany

⁵ Postgraduate Program in Aerospace Engineering, Federal University of Maranhão, Maranhão, Brazil

⁶ Laboratory of Controls and Systems, Federal University of Pará, Pará, Brazil

⁷  0000-0002-8106-0560, Postgrad. Prog. in Electrical Engineering, Federal University of Pará, Pará, Brazil,

*corresponding author: asilveira@ufpa.br

Keywords: satellite launch vehicle, model predictive control, attitude control, flight dynamics, VLS-1.

Abstract: This paper presents the main results of a case study on the attitude control of a satellite launch vehicle using a novel model predictive control (MPC). Control systems design and simulations were based on the model of the Brazilian VLS-1 launcher during the maximum dynamic pressure regime. Such a model was characterized by a 16th-order state-space realization with asymmetrical and coupled attitude dynamics, bending modes, non-collocated sensor-actuator, actuator saturation, wind disturbances, and sensor noise. The idea was to recreate, from a Control Theory perspective, a scenario similar to the 1999 explosion of the VLS-1 V02, which occurred 56 seconds after liftoff, exploring the thesis that the intense vibratory regime could have contributed to the failure. We demonstrate that when non-collocated sensor-actuator and measurement noise are introduced into the simulations, the control-loop performance degrades. In some cases, stability may be lost with commonly practiced control systems technologies, such as Proportional-Integral-Derivative-based controllers. To overcome such problems, we propose and investigate the following MPC technology: Predictive Minimum Variance Control (PMVC) with Full State-Feedback. The adopted methodology inherits the advantages of Linear Quadratic Gaussian, and adds the enhancements of predictive control to mitigate the effects of time delays due to non-collocated sensor-actuator plus processing dead times. The main results were compared to those obtained by applying the PI-D controller once designed for the real VLS-1 launcher. The studied MPC technique was able to guarantee stability and performance where the PI-D failed.

ID number: IIICAB-12

1 Introduction

In this work, a novel model predictive control (MPC) method is proposed and investigated in the problem of attitude control of a satellite launch vehicle based on the Brazilian rocket known as VLS-1. In this study, we investigate the thesis presented by Palmerio 2017, p. 29, that the failure of the VLS-1 launched in 1999 could have been caused by the intense vibratory regime. The considered simulation

model was based on the maximum dynamic pressure state space realization described by Ramos 2011, p. 99-101, having three-inputs and three-outputs, 16 state variables, coupled dynamics, with added bending modes, actuator saturation, non-collocated sensor-actuator, wind and measurement noise disturbances.

The VLS-1 was the first Brazilian satellite launch vehicle project, having three prototypes built and identified by V01, V02, and V03. A fourth version was never finalized, and the project was canceled in 2016 (Silva et al. 2019). The downfall of the VLS-1 project occurred when the V03 exploded in 2003, two days before the launch date, while the vehicle was still inside the assembly building, destroying the facility and killing 21 people who were working at the site.

The V01 was launched in 1997, but one of its four boosters of the 1st-stage did not ignite and the vehicle drifted off-course, generating an increased sideslip angle that led the vehicle to an unbearable aerodynamic stress and rupture, 26 seconds after liftoff (Palmerio 2017). The V02 was launched in 1999 and flew for almost 56 seconds until the engine of its 2nd-stage exploded after ignition (Retro-Space-HD 2022). The V02 endured the maximum dynamic pressure regime, and valuable data became available to enhance the knowledge of the VLS-1 during the intense vibratory regime.

The possible technical cause for the V02 engine explosion was detailed in Palmerio 2017, p. 138. Nonetheless, one thesis added by Palmerio 2017, p. 29, was that the intense vibratory regime could have caused the accident. He remarked that no conclusive proof has been given to support this thesis.

The V02 prototype used attitude controllers structured as PI-D (proportional, integral, *minus* derivative) (Ramos 2011, Silva et al. 2019), that avoids the *derivative kick*, which is an impulsive derivative action due to step-like changes in the attitude references. However, PI-D still differentiates in time noise or attitude angle vibrations and oscillations due to possible undamped bending modes, amplifying these values through the feedback loop to the actuators, leading to excessive control signal chattering and excitation of the bending modes, increased vibrations, and structural damages to the vehicle. Thus, from the Control Theory viewpoint, the thesis raised in Palmerio 2017 is plausible.

The VLS-1 was addressed in the literature as having two bending modes, near 30 and 80 rad/s (cf. Fig. 1 in Sec. 2.1). However, the attitude PI-D controllers' tuning and analysis procedures for the VLS-1 were based on simplified 2nd-order model approximations without the bending modes (Silva et al. 2019).

In Silva et al. 2019, the effects of the bending modes were not taken into consideration, as the authors assumed an ideal attenuation by notch filters. Yamada, Kienitz and Ramos 2024 revisited the attitude control problem of the VLS-1 using a control technology similar to the Linear Quadratic Gaussian (LQG) with Loop-Transfer-Recovery (LTR). They considered the bending modes and, despite stating that the bending modes have been attenuated, in Yamada, Kienitz and Ramos 2024, Fig. 18, the effects of these modes through the feedback loop were still noticeable in the control signals. In their simulations, no vibratory effects (i.e., noise) in the attitude measurements were considered, which could eventually increase the problem. Nonetheless, their LQG based on a more complex design model and controller, has considerably enhanced the robustness and performance of the VLS-1.

Following Yamada, Kienitz and Ramos 2024 footsteps, we propose in this work, for the first time, an LQG-based Predictive Minimum Variance Control with Full State-Feedback (PMVC). The PMVC is a multi-input multi-output MPC technology previously addressed to deal with output-feedback, focusing on minimizing both the tracking error and control signals' power (Silveira et al. 2020). In this new approach, we enhance the PMVC algorithm to full state-feedback to address the minimization of the whole set of state variables at once (Stevens, Lewis and Johnson 2016), including, in a natural and systematic way, the bending modes minimization and stability to non-collocated sensor-actuator delays.

Beyond this introductory part, this work is organized as follows: in Sec. 2, the methodology is presented, comprising the VLS-1 simulation model, the baseline PI-D and its design technique, and the PMVC with full state-feedback proposition. In Sec. 3, the simulation results are shown along with the discussions. The conclusions and ideas for future works are drawn in Sec. 4.

2 Methodology

2.1 VLS-1 Attitude Model

The VLS-1 attitude model considered in this work is based on the work of Ramos 2011, Appendix A. It is defined in the mks unit system (meter, kilogram, second), with angles given in radians. However, all the results presented in this work are shown in degrees due to conversions from radians.

The attitude angles, roll (ϕ), pitch (θ), yaw (ψ), in the body coordinate system, X_b , Y_b , Z_b , respectively aligned Up-East-South, have positive angular rotations around these axes by considering right-handed rotations.

The continuous-time state-space realization for the VLS-1 attitude model is as follows:

$$\dot{\mathbf{x}}(t) = \mathbf{A}_c \mathbf{x}(t) + \mathbf{B}_c \text{sat}[\mathbf{u}(t - t_d)] + \mathbf{G}_c \mathbf{w}(t), \quad (1)$$

$$\mathbf{y}(t) = \mathbf{C} \mathbf{x}(t) + \mathbf{v}(t), \quad (2)$$

$$\text{sat}[\mathbf{u}(t)] = \begin{cases} \mathbf{u}_{\max} & \text{if } \mathbf{u}(t) \geq \mathbf{u}_{\max}, \\ \mathbf{u}(t) & \text{if } \mathbf{u}_{\min} < \mathbf{u}(t) < \mathbf{u}_{\max}, \\ \mathbf{u}_{\min} & \text{if } \mathbf{u}(t) \leq \mathbf{u}_{\min}. \end{cases} \quad (3)$$

The state vector $\mathbf{x}(t) \in \mathbb{R}^{16}$ is comprised of the following state variables:

$$\mathbf{x}^T(t) = [w \quad q \quad \theta \quad \theta_{b11} \quad \theta_{b12} \quad \theta_{b21} \quad \theta_{b22} \quad v \quad r \quad \psi \quad \psi_{b11} \quad \psi_{b12} \quad \psi_{b21} \quad \psi_{b22} \quad p \quad \phi]. \quad (4)$$

v , and w , are the linear velocity components relative to Y_b and Z_b ; p , q , and r , the angular velocities relative to rotations about X_b , Y_b , and Z_b ; θ_{b11} , and θ_{b21} , the 1st and 2nd bending modes of $\theta(t)$; θ_{b12} , and θ_{b22} , the time-derivative of the 1st and 2nd bending modes of $\theta(t)$; ψ_{b11} , and ψ_{b21} , the 1st and 2nd bending modes of $\psi(t)$; ψ_{b12} , and ψ_{b22} , the time-derivative of the 1st and 2nd bending modes of $\psi(t)$.

The input vector is $\mathbf{u}^T(t) = [\beta_\theta \quad \beta_\psi \quad \beta_\phi]$ and is related to the nozzle angular deflections in radians. Positive nozzle deflections on β_θ and β_ϕ generate positive rotations on θ and ϕ , while β_ψ operates inversely on ψ . The control actuators have limited nozzle deflections of $\pm 4^\circ$, represented by \mathbf{u}_{\min} and \mathbf{u}_{\max} , and have a transport time delay t_d to simulate non-collocated sensor-actuator dynamics and other processing and communication delays.

The disturbance vector $\mathbf{w}^T(t) = [w_\theta \quad w_\psi]$ is an input vector, related to wind disturbances given in meters per second, affecting predominantly the pitch and yaw. The sensor-measured output vector is $\mathbf{y}^T(t) = [\theta \quad \psi \quad \phi]$, given in radians, and the sensor noise vector is $\mathbf{v}^T(t) = [v_\theta \quad v_\psi \quad v_\phi]$, simulated as Gaussian noises to assume the worst possible scenario where the whole measurable disturbance spectrum is excited with the same power.

The system matrices, \mathbf{A}_c , \mathbf{B}_c , \mathbf{G}_c , \mathbf{C} , are parameterized as shown in Ramos 2011, Appendix A, but with enabled bending modes by modifying the following elements of the \mathbf{A}_c matrix: $a_{3,4}$, $a_{3,6}$, $a_{10,11}$, $a_{10,13}$, changing their values from 0 to 1.

To design and analyze the digital attitude controllers, it was used the zero-order hold equivalent state-space realization in the discrete time domain k , as follows:

$$\mathbf{x}(k) = \mathbf{A} \mathbf{x}(k-1) + \mathbf{B} \text{sat}[\mathbf{u}(k-d)] + \mathbf{G} \mathbf{w}(k-1), \quad (5)$$

$$\mathbf{y}(k) = \mathbf{C} \mathbf{x}(k) + \mathbf{v}(k). \quad (6)$$

The total discrete time delay is the positive integer $d = 1 + \lceil t_d/T_s \rceil$, with the ceiling operator $\lceil \cdot \rceil$ used to round up to an integer in the case of a fractional relation between t_d and the sampling time T_s .

The sampling time for the digital attitude controllers in this work must safely incorporate the 2nd-bending mode frequency at 80.4 rad/s, or $f_h = 12.796$ Hz.

The rule of thumb shown in Stevens, Lewis and Johnson 2016, p. 601, for aircraft control system design, is $T_s \leq 1/(4f_h)$. Since the VLS-1 is more critical due to its natural open-loop instability, it was considered an even safer rule: $T_s \leq 1/(10f_h)$. Thus, a $T_s = 5$ milliseconds was selected.

In Fig. 1, the magnitude plots of the principal gains for pitch, yaw, and roll, of the continuous- and discrete-time models of the VLS-1 are shown. It is possible to observe that both resonant peaks

of the bending modes are well represented by the discrete-time equivalent model to be used for control system design.

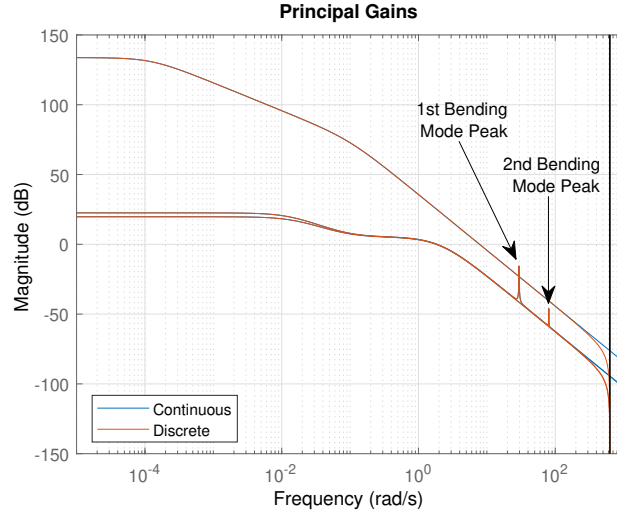


Figure 1: VLS-1 principal gains, remarking the two bending modes at 29.5 and 80.4 rad/s. The discrete-time model obtained using a sampling time of $T_s = 5$ milliseconds can represent the continuous system principal gains for the whole sampled spectrum.

2.2 VLS-1 PI-D Attitude Controllers

The PI-D controller is as follows:

$$U(s) = \left(k_p + k_i \frac{1}{s} \right) R(s) - \left(k_p + k_i \frac{1}{s} + k_d s \right) Y(s), \quad (7)$$

with k_p , k_i , k_d , the proportional, integral, and derivative gains, and $U(s)$, $R(s)$, $Y(s)$, the control, the reference, and the controlled output signals, respectively. This control structure uses a PI to deal with the reference tracking and a PID to deal with the output regulation.

The VLS-1 PI-D tuning and performance were based on the Linear Quadratic Regulator (LQR) method and simplified 2nd-order models as follows (Ramos 2011, Appendix A):

$$\frac{\theta(s)}{\beta_\theta(s)} = \frac{-\bar{M}_{\beta_z}}{s^2 - \bar{M}_\alpha} = \frac{-(-7.3734)}{s^2 - (4.077)}, \quad (8)$$

$$\frac{\psi(s)}{\beta_\psi(s)} = \frac{\bar{N}_{\beta_y}}{s^2 - \bar{N}_\beta} = \frac{(-7.5648)}{s^2 - (4.0726)}, \quad (9)$$

$$\frac{\phi(s)}{\beta_\phi(s)} = \frac{\bar{L}_{\beta_x}}{s^2 + \bar{L}_p s} = \frac{(61.0492)}{s^2 + (0.098859)s}. \quad (10)$$

The relation between the LQR gain and the PI-D gains, when adopting the design method presented by Silva et al. 2019, is as follows:

$$\mathbf{K} = \begin{bmatrix} k_p & k_d & -k_i \end{bmatrix}. \quad (11)$$

By using LQR's optimization weighting matrices as specified by Silva et al. 2019, with $\mathbf{Q} = \text{diag} \begin{pmatrix} 0.1 & 1 & 0.2 \end{pmatrix}$ and $\mathbf{R} = 0.4$, the following gains for the pitch, yaw, and roll were obtained:

$$\begin{aligned} \mathbf{K}_\theta &= \begin{bmatrix} 2.3009 & 1.7675 & -0.7071 \end{bmatrix}, \\ \mathbf{K}_\psi &= \begin{bmatrix} -2.2793 & -1.7614 & 0.7071 \end{bmatrix}, \\ \mathbf{K}_\phi &= \begin{bmatrix} 1.5840 & 1.5958 & -0.7071 \end{bmatrix}. \end{aligned} \quad (12)$$

The discrete time implementation of the PI-D used in this work was obtained using Euler's backward approximation method (Astrom and Wittenmark 2011).

2.3 PMVC with Full State-Feedback

The proposition of a PMVC with Full State-Feedback assumes the predicted state-feedback control law of the form:

$$\Lambda \Delta \mathbf{u}(k) = \mathbf{K} [\mathbf{r}(k) - \hat{\mathbf{x}}_{\mathbf{a}}(k + N_x)], \quad (13)$$

in which $\Delta \mathbf{u}(k) = \mathbf{u}(k) - \mathbf{u}(k - 1)$, Λ is a diagonal matrix for control effort weighting, \mathbf{K} is a state-feedback gain matrix, $\mathbf{r}(k)$ is a vector of state-reference signals and $\hat{\mathbf{x}}_{\mathbf{a}}(k + N_x)$ is the prediction of N_x -steps in the future of the augmented state vector to add discrete integrators to the system inputs:

$$\mathbf{x}_{\mathbf{a}}^T(k) = [\mathbf{y}(k) \quad \Delta \mathbf{x}(k)]. \quad (14)$$

Then, PMVC optimization problem with full state-feedback is reformulated as follows:

$$\min_{\Delta \mathbf{u}(k)} J = \mathbf{E} [\mathbf{g}^T(k + N_x) \mathbf{g}(k + N_x)], \quad (15)$$

$$\mathbf{g}(k + N_x) = \Lambda \Delta \mathbf{u}(k) + \mathbf{K} \hat{\mathbf{x}}_{\mathbf{a}}(k + N_x) - \mathbf{K} \mathbf{r}(k), \quad (16)$$

subject to the augmented system realization with new matrices $\mathbf{A}_{\mathbf{a}}$, $\mathbf{B}_{\mathbf{a}}$, $\mathbf{G}_{\mathbf{a}}$, $\mathbf{C}_{\mathbf{a}}$:

$$\begin{aligned} \begin{bmatrix} \mathbf{y}(k) \\ \Delta \mathbf{x}(k) \end{bmatrix} &= \begin{bmatrix} \mathbf{I} & \mathbf{C} \mathbf{A} \\ \mathbf{0} & \mathbf{A} \end{bmatrix} \begin{bmatrix} \mathbf{y}(k-1) \\ \Delta \mathbf{x}(k-1) \end{bmatrix} + \begin{bmatrix} \mathbf{C} \mathbf{B} \\ \mathbf{B} \end{bmatrix} \Delta \mathbf{u}(k-d) + \begin{bmatrix} \mathbf{I} & \mathbf{C} \mathbf{G} \\ \mathbf{0} & \mathbf{G} \end{bmatrix} \begin{bmatrix} \Delta \mathbf{v}(k) \\ \Delta \mathbf{w}(k-1) \end{bmatrix}, \\ \mathbf{y}_{\mathbf{a}}(k) &= [\mathbf{C} \quad \mathbf{0}] \begin{bmatrix} \mathbf{y}(k) \\ \Delta \mathbf{x}(k) \end{bmatrix}. \end{aligned} \quad (17)$$

The solution to the problem in (15) requires the PMVC state predictor (Silveira et al. 2020):

$$\begin{aligned} \hat{\mathbf{x}}_{\mathbf{a}}(k + N_x) &= \left(\mathbf{A}_{\mathbf{a}}^{N_x} - \mathbf{A}_{\mathbf{a}}^{(N_x-1)} \mathbf{L} \mathbf{C}_{\mathbf{a}} \right) \bar{\mathbf{x}}_{\mathbf{a}}(k) + \mathbf{B}_{\mathbf{a}} \Delta \mathbf{u}(k) \\ &+ \begin{bmatrix} \mathbf{A}_{\mathbf{a}}^1 \mathbf{B}_{\mathbf{a}} \\ \vdots \\ \mathbf{A}_{\mathbf{a}}^{(N_x-1)} \mathbf{B}_{\mathbf{a}} \end{bmatrix}^T \underbrace{\begin{bmatrix} \Delta \mathbf{u}(k-1) \\ \vdots \\ \Delta \mathbf{u}(k - N_x + 1) \end{bmatrix}}_{\underline{\Delta \mathbf{u}(k-1)}} + \mathbf{A}_{\mathbf{a}}^{(N_y-1)} \mathbf{L} \mathbf{y}(k), \end{aligned} \quad (18)$$

$$\bar{\mathbf{x}}_{\mathbf{a}}(k) = (\mathbf{A}_{\mathbf{a}} - \mathbf{L} \mathbf{C}_{\mathbf{a}}) \mathbf{x}_{\mathbf{a}}(k-1) + \mathbf{B}_{\mathbf{a}} \Delta \mathbf{u}(k - N_x) + \mathbf{L} \mathbf{y}(k-1). \quad (19)$$

The matrices \mathbf{K} and \mathbf{L} are LQR and Kalman filter gains of a LQG design, used to “optimally detune” the predictive minimum variance problem.

By solving the optimization problem in (15), the optimal control increment is as follows:

$$\Delta \mathbf{u}(k) = (\mathbf{K} \mathbf{B}_{\mathbf{a}} + \Lambda)^{-1} \left[\mathbf{K} \mathbf{r}(k) - \mathbf{M}_{\mathbf{x}} \bar{\mathbf{x}}_{\mathbf{a}}(k) - \mathbf{M}_{\mathbf{u}} \underline{\Delta \mathbf{u}}(k-1) - \mathbf{M}_{\mathbf{y}} \mathbf{y}(k) \right], \quad (20)$$

$$\begin{aligned} \mathbf{M}_{\mathbf{x}} &= \mathbf{K} \left(\mathbf{A}_{\mathbf{a}}^{N_x} - \mathbf{A}_{\mathbf{a}}^{(N_x-1)} \mathbf{L} \mathbf{C}_{\mathbf{a}} \right), \\ \mathbf{M}_{\mathbf{u}} &= \mathbf{K} \begin{bmatrix} \mathbf{A}_{\mathbf{a}}^1 \mathbf{B}_{\mathbf{a}} & \cdots & \mathbf{A}_{\mathbf{a}}^{(N_x-1)} \mathbf{B}_{\mathbf{a}} \end{bmatrix}, \\ \mathbf{M}_{\mathbf{y}} &= \mathbf{K} \mathbf{A}_{\mathbf{a}}^{(N_x-1)} \mathbf{L}, \end{aligned} \quad (21)$$

and the incremental control law is given by: $\mathbf{u}(k) = \mathbf{u}(k-1) + \Delta \mathbf{u}(k)$.

3 Results and Discussion

In this section, we present a 50-second simulation of the VLS-1 while executing pitch-over and roll program maneuvers based on the guidance data shown by Yamada, Kienitz and Ramos 2024, Fig. 16, with wind disturbances of 6 m/s during liftoff, and 20 m/s 10 seconds later.

For the sake of compactness, just a single and standardized tuning of the PMVC was used: $N_x = 11$, $\Lambda = \mathbf{I}_3$, LQR $\mathbf{Q} = \mathbf{C}_a^T \mathbf{C}_a$ and $\mathbf{R} = 10^3 \mathbf{I}_3$, Kalman filter $\mathbf{Q} = \mathbf{I}_{19}$ and $\mathbf{R} = \mathbf{I}_3$. Theoretically, with the defined state-prediction horizon N_x , the controller would guarantee the closed-loop stability up to $t_d = 50$ ms. Effectively, despite not being shown, the PMVC handled up to $t_d = 120$ ms with $N_x = 11$.

Figure 2 presents the results from simulations with vibrations being captured by the attitude sensors. The variance of the used noises was 10^{-10} . These noises were barely visible in the graphics of the attitude angles, but the control signals, on the other hand, have shown excessive chattering, saturation, and eventually loss of control.

In Fig. 3, the effects of non-collocated sensor-actuator and time delays are shown. It was found that the PI-D would lose stability if $t_d \geq 10$ milliseconds. Figure 3 depicts the case with $t_d = 20$ ms, since the visual impact of this result is stronger, in terms of the PI-D instability.

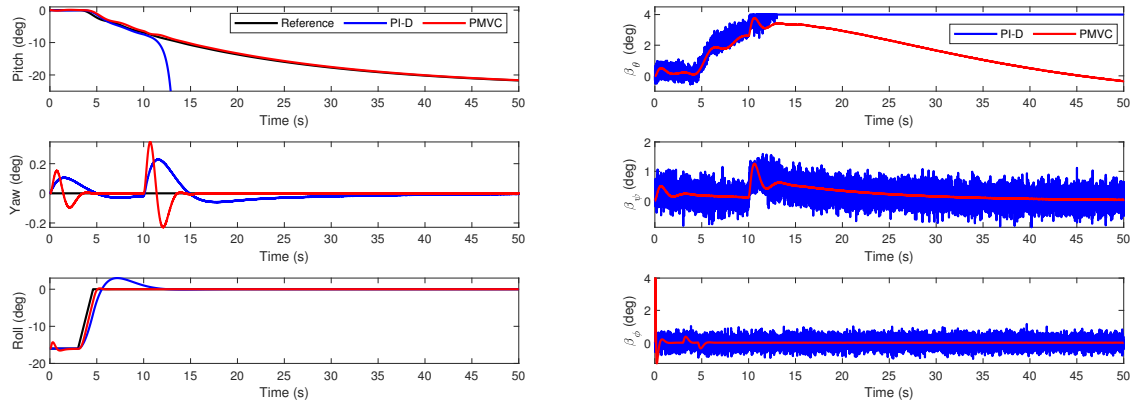


Figure 2.: Attitude angles on the left graphics and control signals on the right. The vibrations simulated with noises linear power of $\sigma_v^2 = 10^{-10}$ were barely visible, but their effect due to feedback in the PI-D was catastrophic, leading to high control signal chattering, saturation, and instability.

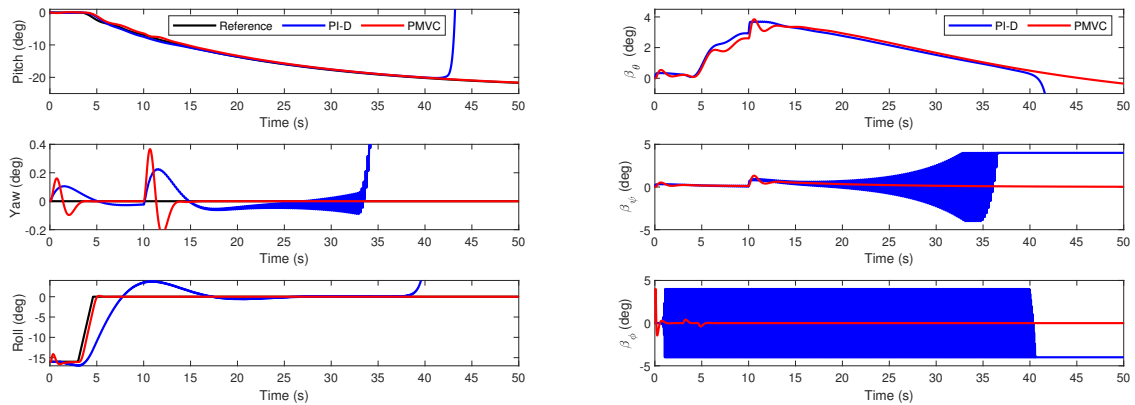


Figure 3.: Attitude angles on the left graphics and control signals on the right. Results for simulated non-collocated sensor-actuator and time delays. Instability with the PI-D was observed for $t_d \geq 10$ ms, but this case in the graphics was simulated using $t_d = 20$ ms, to better depict the problem.

4 Conclusions

In this work, we have investigated the effects of vibrations and time delays acting on the VLS-1 control systems. The non-linear simulation model considered the attitude dynamics during the maximum dynamic pressure phase, with bending modes enabled and actuator saturation. The main results were the difficulties the PI-D controller had when dealing with noises and delays that led to instability, and the successful management of such a complex scenario with the PMVC with full state-feedback.

Even though the PMVC used a much more complex design model, it solves the control problem at once for all state variables, and runs faster than the three independent PI-D controllers. The PMVC simulated loop-time required $0.23545 \mu\text{s}$, and the PI-D $5.5674 \mu\text{s}$. These were the average times after processing 10001 iterations using MATLAB R2021a, using an AMD Ryzen 5 5600 processor, with 32 GB DDR4 at 3200 MHz.

Despite this work cannot bring conclusive proof regarding the thesis added by Palmerio 2017, that the intense vibratory regime was related to the accident with the VLS-1 in 1999, it does bring evidence that the PI-D used in the vehicle lacked the robustness to deal with the vibrations. In a follow-up work, this lack of robustness will be detailed using gain and phase margins, showing from a closed-loop sensitivity analysis perspective that these margins were smaller than expected and how LQG- and MPC-based techniques are by far more appropriate to handle such problems.

4.1 Declaration of Competing Interest

The authors declare no conflict of interest.

References

- Astrom and Wittenmark 2011 ASTROM, K. J.; WITTENMARK, B. *Computer-controlled systems: theory and design*. 3rd. ed. Mineola, NY, USA: Dover Publications, 2011.
- Palmerio 2017 PALMERIO, A. F. *Introdução à Tecnologia de Foguetes*. 2nd. ed. SindCT, São José dos Campos - SP, 2017. Disponível em: <<https://sindct.org.br/sindct/comunicacao/livros-e-cartilhas/introducao-a-tecnologia-de-foguetes/>>.
- Ramos 2011 RAMOS, F. de O. *Automation of H_∞ controller design and its observer-based realization*. Tese (Doutorado) — Instituto Nacional de Pesquisas Espaciais (INPE), Institut Supérieur de l'Aéronautique et de l'Espace (ISAE), São José dos Campos (Brasil), Toulouse (França), 2011.
- Retro-Space-HD 2022 RETRO-SPACE-HD. VLS-1 V2 Launch Failure - Solid Fuel Brazilian Rocket, 1999, Alcantara Space Center. 2022. Disponível em: <<https://www.youtube.com/watch?v=6kx7EHqtG6Q>>.
- Silva et al. 2019 SILVA, F. O. et al. Tuning techniques evaluation for satellite launch vehicle attitude controllers. *Journal of Aerospace Technology and Management*, Dept. of Aerospace Science and Technology, v. 11, p. e2419, 2019. ISSN 2175-9146. Disponível em: <<https://doi.org/10.5028/jatm.v11.1004>>.
- Silveira et al. 2020 SILVEIRA, A. et al. Design and real-time implementation of a wireless autopilot using multivariable predictive generalized minimum variance control in the state-space. *Aerospace Science and Technology*, v. 105, p. 106053, 2020. ISSN 1270-9638.
- Stevens, Lewis and Johnson 2016 STEVENS, B. L.; LEWIS, F. L.; JOHNSON, E. N. *Aircraft Control and Simulation: dynamics, controls design, and autonomous systems*. 3rd. ed. Hoboken, NJ, USA: John Wiley & Sons, Inc., 2016.
- Yamada, Kienitz and Ramos 2024 YAMADA, A. F. C. de S.; KIENITZ, K. H.; RAMOS, F. de O. Robust attitude control of a flexible launch vehicle subjected to wind disturbances. In: *XXV Brazilian Congress of Automatics (CBA), Rio de Janeiro, RJ, Brazil*. [S.l.: s.n.], 2024.